



Università degli Studi Mediterranea di Reggio Calabria
Archivio Istituzionale dei prodotti della ricerca

Collapse load of composite laminates: lower bound evaluation by stress field analytical approximation

This is the peer reviewed version of the following article:

Original

Collapse load of composite laminates: lower bound evaluation by stress field analytical approximation / Bouabid, A., De Domenico, D., Pisano, A.A., Limam, O.. - In: COMPOSITES. PART B, ENGINEERING. - ISSN 1359-8368. - 75:(2015), pp. 345-354. [10.1016/j.compositesb.2015.01.041]

Availability:

This version is available at: <https://hdl.handle.net/20.500.12318/1811> since: 2021-01-19T09:20:15Z

Published

DOI: <http://doi.org/10.1016/j.compositesb.2015.01.041>

Terms of use:

The terms and conditions for the reuse of this version of the manuscript are specified in the publishing policy. For all terms of use and more information see the publisher's website

Publisher copyright

This item was downloaded from IRIS Università Mediterranea di Reggio Calabria (<https://iris.unirc.it/>) When citing, please refer to the published version.

(Article begins on next page)

Collapse load of composite laminates: lower bound evaluation by stress field analytical approximation

Anissa Bouabid¹, Dario De Domenico², Aurora Angela Pisano^{2*}, Oualid Limam¹

¹*Laboratoire de Génie Civil, Ecole Nationale d'Ingénieurs de Tunis,
University of Tunis El Manar, BP 37, 1002 le Belvédère, Tunis, Tunisia*

²*Department PAU, University Mediterranea of Reggio Calabria via Melissari,
I-89124 Reggio Calabria, Italy*

**Corresponding author. Tel.: +39 0965 385219; fax: +39 0965 385217.
E-mail address: aurora.pisano@unirc.it*

ABSTRACT

The paper proposes a limit analysis approach to define the ultimate load capacity of orthotropic composite laminates under biaxial loading and plane stress conditions. A lower bound to the collapse load multiplier is computed by solving a maximization nonlinear problem, according to the static theorem of limit analysis. To set up the optimization problem a stress field distribution is hypothesized at lamina level, moreover inter-lamina stresses are also considered. The effectiveness and validity of the proposed approach is shown by comparing the obtained numerical predictions both with available experimental data and with other numerical results carried out by means of a different numerical lower bound approach.

KEY WORDS: A. Laminates, C. Numerical Analysis, Limit Analysis, Nonlinear Optimization.

1. INTRODUCTION

Composite materials, due to their mechanical and physical properties, are nowadays increasingly used in many advanced engineering fields such as aeronautical, marine and civil engineering. This justifies the continuing scientific interest both in theoretical and experimental studies of such materials. Among the various problems faced on the subject, a paramount effort has been made to determine the ultimate strength of composite laminates to be used for design purposes. However, because of anisotropy and heterogeneity of composite laminates it is difficult to predict strengths. On the other hand, a failure process in a laminate can arise with different failure modes due to matrix crushing, fiber rupture, fiber buckling, delamination and/or a combination of the above phenomena [1]. Furthermore, the failure process is also influenced by the laminate lay-up, the number of layers, their orientation and stacking sequence.

Due to the complexity of the problem, several predicting failure theories for composite laminates have been developed in literature [2]. Some theories are based on linear or nonlinear analysis, some involve damage and/or fracture mechanics concepts, some are applied at lamina level others are applied on a homogenized laminate, some are based on analytical models others on numerical analysis, some others are physically based (see e.g. [3]-[5]). The list is not exhaustive and is out of the scope of this paper to provide an overview on the subject.

About ten different theories of predicting failure in a laminate were compared by Soden et al. [6], [7] by analyzing the results of the *Word Wide Failure Exercise* (WWFE) that remains an open benchmark for those who want to validate a failure theory on composite laminates.

Besides theories presented in [2], among others, a valid alternative to predict the strength capability of a composite laminate is given by the application of nonstandard limit analysis. The nonstandard limit analysis approaches are based on the Radenkovic static and kinematic theorems of limit analysis [8] and allow to evaluate a lower and an upper bound to the collapse load multiplier of a composite laminate in a *direct manner*, i.e. without carrying out a complete post-elastic analysis of stress or strain in the laminate, so resulting relative simple methods of practical connotation for design purposes. It is worth noting that, consistently with a limit analysis theory, these approaches do not allow to describe phenomena arising after a state of incipient collapse such as delamination, debonding or damage in a wider sense.

Despite the above observation, several limit analysis approaches, in the field of composite material structures, have been recently proposed in many scientific contributions and with different scopes. Among others, some studies provided the explicit analytical form of the upper bound multiplier for composite plates in tension [9] or in bending [10] by minimizing the expression of an appropriately derived dissipation power. Other studies are mainly devoted to the determination of plasticity/strength domains for composites. In [11] for example, by using the

homogenization method of periodic media, the plasticity domain of metal matrix composites is found by solving a limit analysis problem on a unit cell. Papers [12] and [13] are aimed at determining the plasticity domain of composite laminates and pin-loaded composite laminates, respectively, under a tensile loading; in these contributions the laminate is modelled as a three-dimensional solid and the problem is solved by combining finite element methods and mathematical programming numerical procedures. As an alternative approach, limit state solutions may be obtained from sequences of elastic (linear) analyses of the structure. In this case the elastic parameters of the constituent materials of the structure are suitably changed to mimic inelastic phenomena. In particular, to this kind of approach belong the Linear Matching Method (LMM) and the Elastic Compensation Method (ECM). The former is a procedure aimed at constructing a collapse mechanism for the evaluation of an upper bound, while the second is a procedure aimed to constructing an admissible stress field suitable for the evaluation of a lower bound. Both procedures have been recently applied in the field of composite materials to determine the load bearing capacity of multi-layers composite laminates and pin-loaded structural elements (see e.g. [14]-[19]).

Finally, a broad overview of the state of the art concerning numerical and theoretical developments of direct methods can be found in the books [21]-[23] and references therein, which collect the results of international workshops on this topic.

In the context of limit analysis procedures may be inserted the present paper which proposes a lower bound approach to predict the strength capability of orthotropic composite laminates under biaxial loading and plane stress conditions. In particular, the implemented procedure considers a multilayered domain which is a 3D cylindrical domain. Each layer obeys, by hypothesis, a Tsai-Wu type criterion [23] and, in particular, a second order polynomial form of it, the latter assumed as yield condition. Moreover, for each layer, a stress field distribution has been hypothesized in such a way that it satisfies boundary conditions and it results in equilibrium with the applied loads. An optimization nonlinear problem is then solved to determine the searched lower bound to the collapse load multiplier.

Four numerical examples are carried out to validate the proposed approach by comparing the obtained results both with experimental data and with the results of another limit analysis approach available in literature. Precisely, the first two examples are aimed to construct a biaxial failure envelope for two multi-layered composite laminates under biaxial loads, the latter are described in detail in the well documented WWFE [6], [7]. The second couple of examples concerns the peak load prediction of a square composite plate having different material configurations and subjected to two different loading conditions, in this case the obtained results are compared with those obtained by Pisano et al. via the elastic compensation method [25]. For all the examined examples, the predicted ultimate

loads appear in good agreement with the expected ones so validating the proposed approach and encouraging for further investigations.

2. LIMIT LOAD OF A COMPOSITE LAMINATE SUBJECTED TO BIAXIAL LOADING – THEORETICAL BACKGROUND

2.1 GEOMETRY AND MECHANICAL MODEL

To model the laminate consisting of n unidirectional plies, a mechanical model was developed for a multilayer domain with n anisotropic layers (Fig. 1). The laminate is designed as a cylindrical domain Ω of \mathbb{R}^3 with a plane base $\omega = [-a/2, a/2] \times [-b/2, b/2] \in \mathbb{R}^2$ and n layers (or plies). Each ply is designed as a cylindrical domain Ω_i with a thickness e^i . The overall thickness of the multilayer laminate is denoted by $h = \sum_{i=1}^n e^i$. In the following, a single bar beneath the symbols denotes a vector, two bars indicate a second order tensor. The set $(\underline{e}_x, \underline{e}_y, \underline{e}_z)$ is an orthogonal vectorial basis of Ω with $(\underline{e}_x, \underline{e}_y) \in \omega$ and $\Omega = \omega \times [0, h]$. The relative cylindrical domains for the different plies are denoted by $\Omega_i = \omega \times [\sum_{i=1}^{i-1} e^i, \sum_{i=1}^i e^i]$ for the layers $i \in \{2, \dots, n\}$ and $\Omega_1 = \omega \times [0, e_1]$ for the layer 1 at the bottom of the laminate. The interface between two adjacent layers i and $i+1$ is represented by the surface $\Omega_i \cap \Omega_{i+1}$ (Fig. 1).

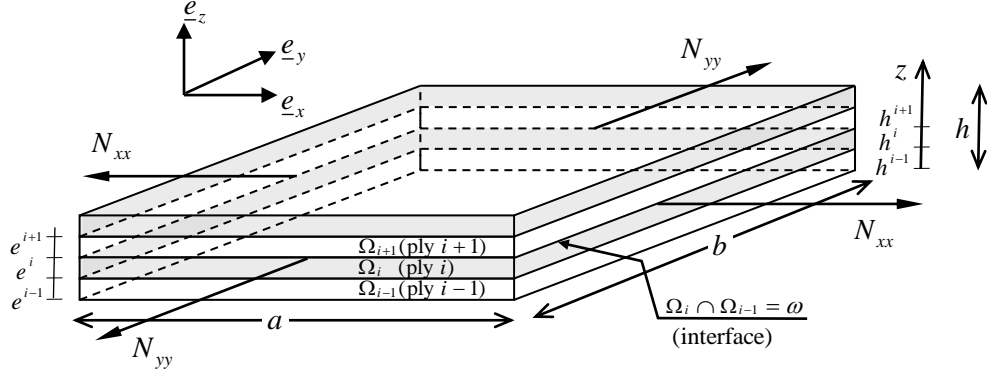


Fig. 1. Schematic mechanical model of a multilayer composite laminate subjected to a biaxial loading condition.

Looking at Fig. 1, a biaxial loading condition is assumed in which membrane loads (N_{xx}, N_{yy}) are applied at the four edges of the laminate, i.e. at $x = \pm a/2$ and $y = \pm b/2$. The membrane loads are defined as:

$$\begin{aligned}
 N_{xx} &= \int_{-\frac{h}{2}}^{\frac{h}{2}} \sigma_{xx} dz = \sum_{i=1}^n \int_{h^{i-1}}^{h^i} \sigma_{xx}^i dz \\
 N_{yy} &= \int_{-\frac{h}{2}}^{\frac{h}{2}} \sigma_{yy} dz = \sum_{i=1}^n \int_{h^{i-1}}^{h^i} \sigma_{yy}^i dz
 \end{aligned} \tag{1}$$

where σ_{xx} and σ_{yy} are the stress values at the edges of the laminate $x = \pm a/2$ and $y = \pm b/2$, respectively. Similarly, σ_{xx}^i and σ_{yy}^i are the stress values at the edges $x = \pm a/2$ and $y = \pm b/2$ in a layer i and h^i indicates the ordinate of the upper face of ply i or, equivalently, of the lower face of ply $i+1$, see again Fig. 1.

2.2 STRESS TENSOR, EQUILIBRIUM EQUATIONS AND BOUNDARY CONDITIONS

2.2.1 STRESS TENSOR

The second order stress tensor is written in Ω_i , the field related to ply i , as follows:

$$\underline{\underline{\sigma}}^i(\underline{X}) = [\sigma_{\alpha\beta}^i(\underline{X})] \quad \text{where } \underline{X} = (x, y, z), i \in \{1 \dots n\} \quad \text{and } \alpha, \beta \in \{x, y, z\} \quad (2)$$

Because of the symmetry of geometry, loading and boundary conditions, the study can be limited to a quarter of the laminate, i.e. only the domain $(x, y) \in [0, a/2] \times [0, b/2]$ is analyzed. We assume $\sigma_{xx}^i(\underline{X})$ and $\sigma_{yy}^i(\underline{X})$ to be linear functions of x and y , respectively, and satisfying the boundary conditions at the edges. The tangential stress components $\sigma_{xy}^i(\underline{X})$ are taken constant per ply i , i.e.:

$$\begin{cases} \sigma_{xx}^i(\underline{X}) = \sigma_{xx0}^i + \frac{\sigma_{xx}^i - \sigma_{xx0}^i}{\frac{a}{2}} x \\ \sigma_{yy}^i(\underline{X}) = \sigma_{yy0}^i + \frac{\sigma_{yy}^i - \sigma_{yy0}^i}{\frac{b}{2}} y \\ \sigma_{xy}^i(\underline{X}) = \sigma_{xy}^i \end{cases} \quad \forall \underline{X} \in \left[0, \frac{a}{2}\right] \times \left[0, \frac{b}{2}\right] \times [h^{i-1}, h^i] \quad (3)$$

in which: σ_{xx}^i and σ_{yy}^i are the stress values at the edges of the plate assumed constant per ply i ; σ_{xx0}^i and σ_{yy0}^i are the stress values at the center of the plate assumed constant per ply i ; σ_{xy}^i are the tangential stress values assumed constant

per ply i . The latter assumption arises from considering the shear stress field to be only caused by the stacking sequence effect across the laminate, i.e., no membrane tangential load is assumed to be applied onto the laminate. Finally, the stresses $\sigma_{xz}^i(\underline{X})$, $\sigma_{yz}^i(\underline{X})$ and $\sigma_{zz}^i(\underline{X})$ are taken as linear functions of z , i.e.:

$$\begin{aligned}\sigma_{xz}^i(\underline{X}) &= \sigma_{xz}^i(z) = \sigma_{xz}^{i-1,i} + (z - h^i) \frac{\sigma_{xz}^{i,i+1} - \sigma_{xz}^{i-1,i}}{e^i} \\ \sigma_{yz}^i(\underline{X}) &= \sigma_{yz}^i(z) = \sigma_{yz}^{i-1,i} + (z - h^i) \frac{\sigma_{yz}^{i,i+1} - \sigma_{yz}^{i-1,i}}{e^i} \\ \sigma_{zz}^i(\underline{X}) &= \sigma_{zz}^i(z) = \sigma_{zz}^{i-1,i} + (z - h^i) \frac{\sigma_{zz}^{i,i+1} - \sigma_{zz}^{i-1,i}}{e^i}\end{aligned}\quad (4)$$

where $\sigma_{xz}^{i,i+1}$, $\sigma_{yz}^{i,i+1}$ and $\sigma_{zz}^{i,i+1}$ are the inter-laminar stress values. Moreover, stresses given in (4) must satisfy the boundary conditions, the stress vector continuity conditions at each lamina interface and the local equilibrium equations for $z \in [h^{i-1}, h^i]$ as better specified in the next section.

2.2.2 EQUILIBRIUM EQUATIONS AND BOUNDARY CONDITIONS

The stress field previously selected must satisfy the local equilibrium given by the following Eq. (5) for volume forces equal to zero, the boundary conditions at $x = a/2$ and $y = b/2$ derived from Eq.(1), the free edge conditions on the top and bottom face of the laminate, Eq. (7) (at $z = 0$ and $z = h^n$, respectively), and the stress vector continuity at the interface ω (see Eq. (8)) must also be satisfied.

$$\text{div} \underline{\underline{\sigma}}^i = \underline{0} \quad (5)$$

$$p_{xx} = \frac{N_{xx}}{h} = \frac{1}{h} \sum_{i=1}^n (e^i \sigma_{xx}^i) \quad ; \quad p_{yy} = \frac{N_{yy}}{h} = \frac{1}{h} \sum_{i=1}^n (e^i \sigma_{yy}^i) \quad (\text{at the edges}) \quad (6)$$

$$\underline{\underline{\sigma}}^n \cdot (\underline{e}_z) = \underline{0} \quad ; \quad \underline{\underline{\sigma}}^1 \cdot (-\underline{e}_z) = \underline{0} \quad (\text{on the top and bottom face of the laminate}) \quad (7)$$

$$\sigma_{\alpha z}^i(x, y, h_i) = \sigma_{\alpha z}^{i+1}(x, y, h_i), \quad \alpha \in \{x, y, z\} \quad (8)$$

In the above equations p_{xx} and p_{yy} are the weighted average values (across all the layers) of the σ_{xx} and σ_{yy} stresses calculated at the edges $x=a/2$ and $y=b/2$, respectively. Note that the condition given in Eq. (8) is naturally satisfied by the choice of the stress field given by Eq.(4). Similarly to Eqs. (1), membrane tangential loads N_{xy} may be defined as follows:

$$N_{xy} = \int_{-\frac{h}{2}}^{\frac{h}{2}} \sigma_{xy} dz = \sum_{i=1}^n \int_{h_{i-1}}^{h_i} \sigma_{xy}^i dz = \sum_{i=1}^n (h^{i-1} - h^i) \sigma_{xy}^i = \sum_{i=1}^n e^i \sigma_{xy}^i. \quad (9)$$

In case of no membrane tangential loads acting on the laminate, as in Fig. 1, the tangential stress σ_{xy}^i in each ply i must satisfy the condition:

$$\sum_{i=1}^n e^i \sigma_{xy}^i = 0 \quad (10)$$

that, for laminates having layers of equal thicknesses, reduces to

$$\sum_{i=1}^n \sigma_{xy}^i = 0. \quad (11)$$

2.3 FAILURE CRITERION IN LAYERS

In Fig. 2, $(\underline{e}_1^i, \underline{e}_2^i, \underline{e}_z)$ represents the layer local co-ordinate system where \underline{e}_1^i is in the longitudinal direction of fibers, \underline{e}_2^i is in the transversal direction to fibers and $\underline{e}_3 \equiv \underline{e}_z$ is in the orthogonal direction to the loading plane. In a ply i , the fiber orientation angle is denoted by θ_i .

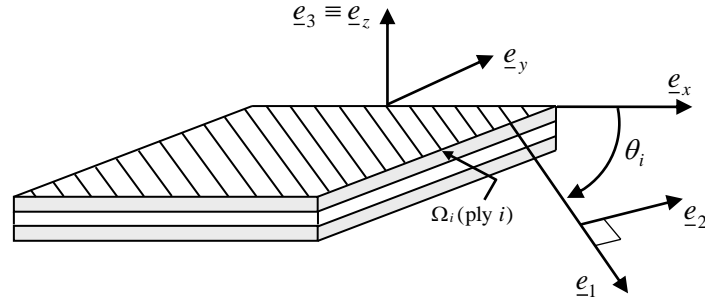


Fig. 2. Local and global coordinate systems for a multi-layered laminate.

For anisotropic materials Tsai and Wu [23] proposed a (failure) criterion in a tensor polynomial form, which, for the case of a unidirectional orthotropic laminate under plane stress conditions, is written as:

$$F_1\sigma_1 + F_2\sigma_2 + F_6\sigma_6 + F_{11}\sigma_1^2 + F_{22}\sigma_2^2 + F_{66}\sigma_6^2 + 2F_{12}\sigma_1\sigma_2 = 1. \quad (12)$$

In Eq. (12) F_i and F_{ij} (with $i, j = 1, 2, 6$) are strength tensors of the second and fourth rank, respectively; 1 and 2 denote the principal directions of orthotropy in plane stress case [1].

The coefficients F_i and F_{ij} ($i, j = 1, 2, 6$) have to be determined by tensile, compressive and shear tests and are functions of the longitudinal tensile and compressive strengths (X_t and X_c), of the transverse tensile and compressive strengths (Y_t and Y_c) as well as of the longitudinal shear strength S [1], [17]. It is worth remarking that in the present paper the Tsai–Wu type criterion of Eq.(12) is used for defining an admissible stress states domain (see [10], [18]). Points within the domain locate stress states pertaining to an anisotropic linear elastic behavior of the material. Points lying on the domain boundary locate stress states at which the material has exhausted its strength capabilities. Besides being a domain within which the stress state may be designated elastic, Eq. (12) also defines a *convex* domain which is an additional requirement for applying a limit analysis approach as the one proposed in this paper.

As the Tsai–Wu type criterion applies to the local coordinate system $(\underline{e}_1^i, \underline{e}_2^i, \underline{e}_3^i)$ while the other relationships involved in the optimization problem and introduced in the previous sections are referred to the global coordinate system $(\underline{e}_x, \underline{e}_y, \underline{e}_z)$, a transformation rule, which is merely a rotation of stress directions, has to be applied. Only for completeness, we recall from elementary mechanics of materials that for expressing stresses in the (1,2,3) coordinate system in terms of stresses in the (x,y,z) coordinate system, by considering Fig. 2 the following transformation equations are applied at the generic layer i :

$$\begin{bmatrix} \sigma_{11}^i \\ \sigma_{22}^i \\ \sigma_{12}^i \\ \sigma_{13}^i \\ \sigma_{23}^i \\ \sigma_{33}^i \end{bmatrix} = \begin{bmatrix} \cos^2 \theta_i & \sin^2 \theta_i & 2\sin\theta_i\cos\theta_i & 0 & 0 & 0 \\ \sin^2 \theta_i & \cos^2 \theta_i & -2\sin\theta_i\cos\theta_i & 0 & 0 & 0 \\ -\sin\theta_i\cos\theta_i & \sin\theta_i\cos\theta_i & \cos^2 \theta_i - \sin^2 \theta_i & 0 & 0 & 0 \\ 0 & 0 & 0 & \cos\theta_i & \sin\theta_i & 0 \\ 0 & 0 & 0 & -\sin\theta_i & \cos\theta_i & 0 \\ 0 & 0 & 0 & 0 & 0 & 1 \end{bmatrix} \begin{bmatrix} \sigma_{xx}^i \\ \sigma_{yy}^i \\ \sigma_{xy}^i \\ \sigma_{xz}^i \\ \sigma_{yz}^i \\ \sigma_{zz}^i \end{bmatrix} \quad (13)$$

According to the scheme sketched in Fig. 3, biaxial loading conditions for the laminate are assumed by means of a *radial loading path*. An angle α establishes the ratio of load magnitudes in the x and y directions, p_{xx} and p_{yy} , respectively, according to the formula:

$$p_{yy} = \tan \alpha p_{xx} \quad \text{with} \quad \alpha \in [0, 2\pi], \quad (14)$$

where p_{xx} and p_{yy} are the weighted average stresses applied to the edges $x = \pm a/2$ and $y = \pm b/2$, respectively. Expression (14) will be considered as an additional constraint of the optimization limit analysis problem. As will be shown in Section 3.1, the assumption of such radial loading path is particularly suitable for constructing the biaxial failure envelope, because varying the α value throughout the trigonometric circle $[0, 2\pi]$ enables covering all the possible biaxial loading conditions thus describing the complete failure envelope in a straightforward manner. On the other hand, uniaxial load distributions along the x axis (e.g. tractions as the ones assumed in Section 3.2) may be obtained by setting $\alpha=0$ in the maximization problem (i.e. $p_{yy}=0$).

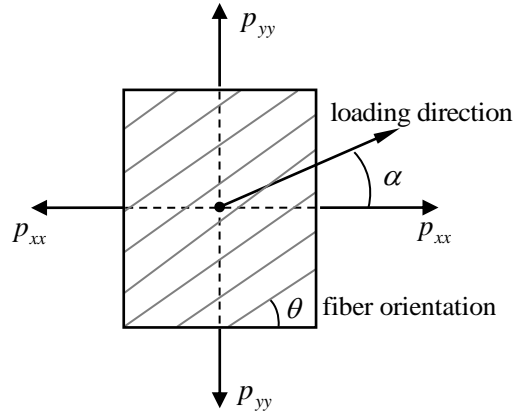


Fig. 3. Schematic model of radial loading path to set biaxial loading conditions for the laminate.

2.4 A LOWER BOUND APPROACH

In order to find the failure load, a lower bound approach of limit analysis is considered. The set of potentially bearable loads must be in equilibrium with a statically admissible (SA) and plastically admissible (PA) stress field. More specifically, a SA stress field must satisfy equilibrium conditions (5) and boundary conditions (6), (7), whereas a PA stress field satisfy the yield criterion (12) at all points within the domain. The class of potentially bearable loads may therefore be expressed by the following set:

$$K^- = \left\{ (p_{xx}, p_{yy}) / \exists (\sigma_{xx}^i, \sigma_{yy}^i, \sigma_{xy}^i, \sigma_{xz}^i, \sigma_{yz}^i, \sigma_{zz}^i) \text{ SA and PA} \right\}. \quad (15)$$

2.5 IMPLEMENTATION OF THE MAXIMIZATION PROBLEM

The present lower bound approach turns out to be a maximization problem to be solved. In particular, the weighted average pressures p_{yy} at the edges (considered as objective function) has to be maximized under the conditions given by the local equilibrium equations, boundary conditions, the coordinate system

transformation, the yield criterion and the loading path. Constraints containing the index i must be written n times for each layer i since each condition is valid at lamina level. The yield criterion must be verified for each ply i and a limit criterion is considered on the inter-laminar shear stresses as follows:

$$|\sigma_{xz}| \leq \tau \quad \text{and} \quad |\sigma_{yz}| \leq \tau, \quad (16)$$

where τ denotes the inter-laminar shear strength. On the basis of the convexity property of the yield criterion (12), it can be demonstrated that the maximization problem written for the studied domain $(x, y) \in [0, a/2] \times [0, b/2]$ is equivalent to the maximization problem written with reference to the four corner points of the laminate only, namely:

$$\begin{aligned} P_1(z) &= P_1(\bar{x} = 0, \bar{y} = 0, z) \\ P_2(z) &= P_2(\bar{x} = 0, \bar{y} = b/2, z) \\ P_3(z) &= P_3(\bar{x} = a/2, \bar{y} = 0, z) \\ P_4(z) &= P_4(\bar{x} = a/2, \bar{y} = b/2, z). \end{aligned} \quad (17)$$

The considered approximation of the stress field reduces the number of variables within the optimization problem to $(9n-3)$ parameters, n being the number of plies.

These parameters are: $\sigma_{xx}^i, \sigma_{yy}^i, \sigma_{xy}^i, \sigma_{xz}^i, \sigma_{yz}^i, \sigma_{zz}^i$ in each ply i ($6n$) and $\sigma_{xz}^{i,i+1}, \sigma_{yz}^{i,i+1}, \sigma_{zz}^{i,i+1}$ in each interface $\Omega_i \cap \Omega_{i+1}$ ($3(n-1)$).

The optimization problem has been solved by using the software Maple [25]. In particular, the algorithm used for the present study is the Sequential Quadratic Programming (SQP) method which is available for arbitrary unconstrained or

constrained nonlinear programs. We recall that the key idea of SQP algorithms is to replace a nonlinear problem, as the one here involved, with a sequence of quadratic sub-problems, in such a way that the sequence of solutions of the sub-problems converges to the solution of the original problem. Each sub-problem is solved by employing a Newton's method (using a quadratic approximation of the objective function subject to a linearization of the constraints) and the solution for a given iteration k is used to construct a new iteration $k+1$ until convergence. Having in mind all the conditions discussed above, the maximization problem is written out as follows:

$$\begin{array}{l}
 \text{Max } p_{yy} \\
 \text{subject to } \left\{ \begin{array}{l}
 \text{Stress field expressions, Eqs. (3), (4)} \\
 \text{Local and global equilibrium equations, Eqs. (5), (10)} \\
 \text{Static boundary conditions, Eqs. (6), (7)} \\
 \text{Stress vector continuity at the interfaces, Eq. (8)} \\
 \text{Failure criterion, Eq. (15) at } P_1(z), P_2(z), P_3(z), P_4(z), z \in [h_{i-1}, h_i], i \in \{1..n\} \\
 \text{Transformation equations, Eq. (13)} \\
 \text{Loading path, Eq. (14)} \\
 \text{Limit criterion on the inter-laminar shear stresses, Eq. (16)}
 \end{array} \right. \quad (18)
 \end{array}$$

3. VALIDATION OF THE PROPOSED MODEL

The applicability and efficacy of the proposed static approach has been scrutinized by comparing the numerical predictions with both experimental findings, available in literature, and numerical results given by another limit analysis approach. In this regard, four different groups of examples have been analyzed and discussed in this section. Examples #1 and #2 concern the construction of a biaxial failure envelope for two multi-layered composite

laminates under biaxial loads. The mechanical properties of these two laminates as well as their complete biaxial failure envelope are well-documented experimentally because these laminates were selected, within a set of six laminate types, as benchmarks in the WWFE [6], [7]. As already said in the introductory section, these benchmarks constitute an important reference for the validation of any failure theory applied to composite laminates.

Examples #3 and #4, on the other hand, concern a square orthotropic plate with a variety of material properties (a parametric study is, in fact, performed) and subjected to two different loading conditions, namely a uniform tension and a uniaxial tensile triangular distribution, respectively. Such square plate was already analyzed via other numerical limit-analysis procedures based on different static and kinematic approaches [18], [9]. Despite the simplicity of the latter two examples, the possibility to compare numerical results obtained by the proposed approach not only with experimental findings but also with results given by alternative limit-analysis-based procedures is, in the authors' opinion, highly important to check the consistency and effectiveness of the proposed procedure in determining the collapse load value for composite laminates.

3.1 EXAMPLES #1 AND #2

As mentioned, the first two examples have been taken from the WWFE [7] and concern a $[\pm 55^\circ]_s$ E-glass/MY750 laminate and a $[90^\circ/\pm 30^\circ]_s$ E-glass/LY556 laminate under biaxial loading conditions (Fig. 4a,b). It has to be noted that the

weighted average stresses p_{xx} and p_{yy} appearing in Fig. 4a,b are coincident with the biaxial stresses σ_x and σ_y , respectively. Full details about the experimental results for the first laminate are presented and discussed in [26]-[28], whereas for the second laminate reference is made to the experimental study performed in [29]. Test results of both the laminate types were systematically summarized in [6]. Different reasons motivated the choice of the aforementioned laminate types in the present study. The first laminate $[\pm 55^\circ]_s$ was selected in the WWFE and analyzed in this paper because of its widespread use in industrial pipework and availability of experimental results on the failure under a broad range of biaxial stresses including those in the compression-compression quadrant [6]. The latter aspect is important to assess the numerical predictive performance of the proposed limit analysis approach with regard to a wide range of loading conditions throughout the biaxial failure envelope σ_x - σ_y . Also the choice of the second laminate $[90^\circ/\pm 30^\circ]_s$ is partly due to the large availability of experimental data on the failure envelope in terms of combined biaxial loads σ_y - σ_x . However, a substantial difference may be recognized between these two lay-up configurations: the $[\pm 55^\circ]_s$ stacking sequence results in a balanced and symmetric angle ply configuration and in a quasi-isotropic laminate, whereas the $[90^\circ/\pm 30^\circ]_s$ stacking sequence lead to a general orthotropic (not quasi-isotropic) laminate; in the latter case the strength depends on the loading direction and a number of different failure modes are therefore expected to be experienced under biaxial loading [6]. Consequently, the construction of the complete biaxial failure

envelope for these two laminates through the static approach discussed in Section 2 guarantees covering a rather general survey of data, being representative of a wide range of failure modes often encountered in industrial practical use, for a careful and thorough inspection of its predictive capabilities.

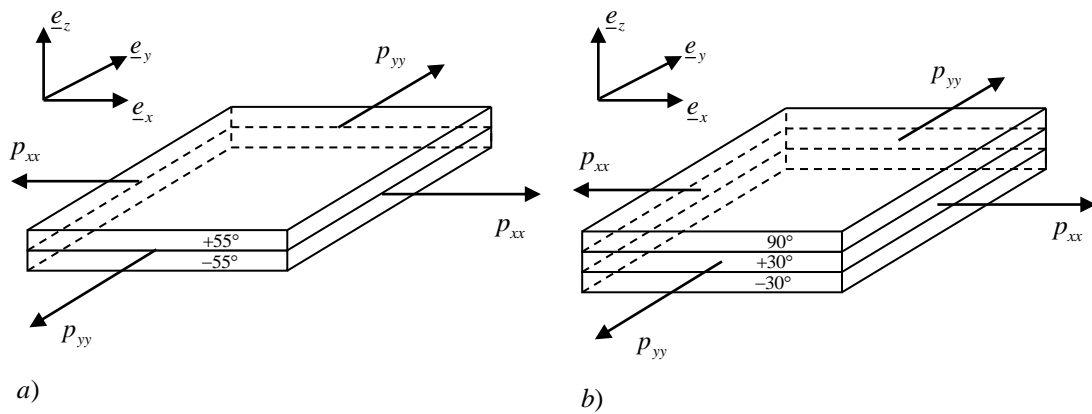


Fig. 4. Mechanical model of example #1 and #2 (only one half of the plate thickness is considered for symmetry reasons): a) $[\pm 55^\circ]_s$ laminate under biaxial load; b) $[90^\circ/\pm 30^\circ]_s$ laminate under biaxial load.

It is worth noting that, due to the difficulties involved in performing experiments on such laminates under a wide range of loading conditions, almost all the experimental results (here considered for comparison purposes) were derived from tests on filament wound glass/epoxy tubular specimens (see [6], [30] for details about experimental equipment). However, this is only an experimental issue (above all, testing on tubes avoids problems associated with free edge effects encountered with other specimen shapes), because there exist well-known relationships that enable a simple conversion of such stress quantities [6], [30]. The laminate tubes were set up from unidirectional fiber reinforced composite

plies, where the ply angle θ was specified as the angle between the fiber direction and the axis of the tube. As a result, $\theta=90^\circ$ corresponds to the circumferential direction $\sigma_\theta \equiv \sigma_y$, whereas $\theta=0^\circ$ leads to an axial stress for the tube $\sigma_a \equiv \sigma_x$. Manifold, specific biaxial loading conditions can therefore be reproduced by performing tests on such tubular specimens under combined axial load (tension or compression), torsion and/or radial pressure (internal or external). On the basis of that, a point in the biaxial failure envelope σ_y - σ_x corresponds to a fixed ratio of circumferential to axial stress σ_θ/σ_a in the experimental counterpart.

Table 1. Example #1 and #2: mechanical parameters of the unidirectional lamina forming the composite laminates

E-glass/MY750 lamina ($[\pm 55^\circ]_s$ laminate)					
Elastic moduli (GPa) and Poisson ratio	E_1	E_2	G_{12}	ν_{12}	
	45.6	16.2	5.83	0.278	
Strength (MPa)	X_t	X_c	Y_t	Y_c	S
	1280	800	40	145	73
E-glass/LY556 lamina ($[90^\circ/\pm 30^\circ]_s$ laminate)					
Elastic moduli (GPa) and Poisson ratio	E_1	E_2	G_{12}	ν_{12}	
	53.5	17.7	5.83	0.278	
Strength (MPa)	X_t	X_c	Y_t	Y_c	S
	1140	570	35	114	72

The mechanical properties of the unidirectional lamina forming the composite laminates are reported in Table 1. The total thickness for the $[\pm 55^\circ]_s$ laminate is 1mm (consequently, the thickness of each lamina is 0.25mm), whereas for the $[90^\circ/\pm 30^\circ]_s$ the total thickness is 2mm (so that the $\pm 30^\circ$ plies cover 82.8% of the total thickness and the 90° plies form the remaining 17.2% of the laminate thickness).

The construction of the biaxial failure envelope for the $[\pm 55^\circ]_s$ E-glass/MY750 composite laminate is illustrated in Fig. 5. Experimental data, superimposed in the plot for comparison purposes, were obtained on tubes having either 100 or 51mm inner diameter and various thicknesses. In particular, results reported in Soden *et al.* [26], [27] were obtained on typically 1mm thick tubes (although a couple of exceptions regarding 5.1mm thick specimens were included too) with 100mm inner diameter and subjected to combined internal pressure and axial loading; on the other hand, experimental data documented in Kaddour *et al.* [28] refer to both 100 and 51mm inner diameter tubes with thicknesses ranging from 4.24mm to 14.4mm. The latter tubular specimens were tested under combined pressure and axial compression [6], [28] and, therefore, give indications on the biaxial failure envelope in the third (compression-compression) quadrant only.

As can be seen in Fig. 5, a reasonably satisfactory correlation of the numerical results with the experimental data is obtained for the $[\pm 55^\circ]_s$ laminate throughout the biaxial failure envelope, that is, for almost all the loading combinations. More in depth, a really good failure estimation is obtained by the lower bound approach both in the biaxial tension-tension and compression-compression quadrants (first and third quadrants). Very few scattered experimental data are present in the fourth (tension-compression) quadrant, however accurate numerical results may be observed also in this zone of the biaxial failure envelope. Finally, there being practically no data in the second (compression-tension) quadrant, no direct

comparison can be made although a likely trend from the contiguous experimental results can be envisaged which, once again, correlates very well with the corresponding numerical prediction.

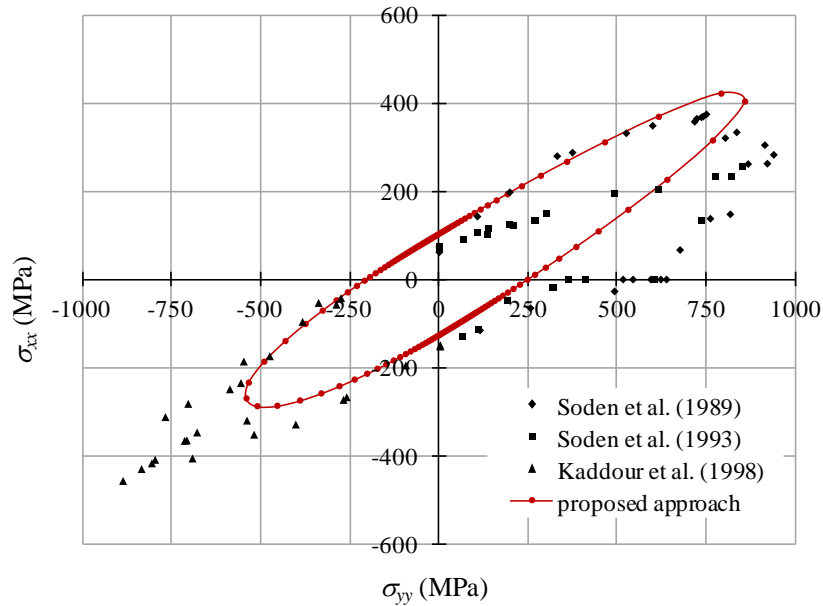


Fig. 5. Example #1: biaxial failure envelope for the $[\pm 55^\circ]_s$ E-glass/MY750 composite laminate (comparison with experimental data after [26], [27], [28]).

On the other hand, the construction of the biaxial failure envelope for the $[90^\circ/\pm 30^\circ]_s$ E-glass/LY556 composite laminate is depicted in Fig. 6. Extensive experimental work on this laminate type was carried out by Hütter *et al.* [29]. Experimental data, superimposed in the plot for comparison purposes, were obtained on tubes 2mm thick and having 60mm inner diameter [29]. Tubes with two external circumferentially wound 90° layers and helically wound $\pm 30^\circ$ central layers were subjected to combined internal pressure (hoop stress) and axial load [6].

Also in this case, a quite accurate numerical prediction of the failure envelope is achieved through the proposed limit analysis approach. Apart from the little deviation observed in the second quadrant (particularly for small σ_y values approaching zero), a rather good description of the failure envelope as a whole can be observed, especially in the biaxial tension-tension and tension-compression (first and fourth) quadrants. Nonetheless, an overestimation of the predicted failure envelope compared to the experimental scattered data can easily be recognized in the third (compression-compression) quadrant. In this regard, it is worth noting that tubular specimens can experience various forms of buckling when they are subjected to combined circumferential or axial compression [6]. Actually, as stated in the related experimental report [29], the few test results carried out under external pressure and axial compression (i.e. in the compression-compression quadrant) were reported to be governed by buckling. This experimental fact may presumably justify the overestimation of the experimental results in the third quadrant. Furthermore, under certain loading conditions, e.g. under high combined tension-tension stresses, delamination between plies may occur at the ends of the tubular configuration [1] and considerable damage may accumulate as well, which may, to some extent, explains some differences observed in the first quadrant.

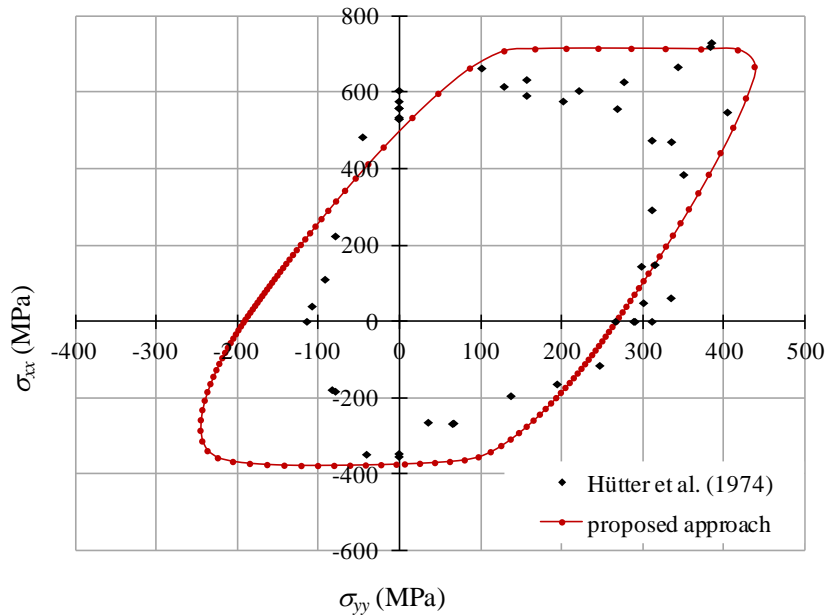


Fig. 6. Example #2: biaxial failure envelope for the $[90^\circ/\pm 30^\circ]_s$ E-glass/LY556 composite laminate (comparison with experimental data after [29]).

3.2 EXAMPLES #3 AND #4

In addition to examples #1 and #2 discussed in the previous section, two further numerical examples have been addressed to verify the effectiveness of the proposed static approach. These are two case studies which were solved numerically by different limit-analysis-based procedures (here only lower bound approaches based on the static theorem have been considered for uniformity with the proposed approach). In particular, example #3 concerns a square plate under plane stress conditions and, by hypothesis, made of a *tetratropic* material (Fig. 7). This example was first studied in [9] by means of an upper bound approach: for this simple problem the actual collapse mechanism, i.e. a uniform strain rate field, is in fact immediately detected and thus the use of the kinematic theorem leads to an explicit analytical expression of the upper bound multiplier [9]. The example

carried out in the above mentioned paper presents an interesting sensitivity analysis on the influence of the ratio between tensile and compressive strength as well as of the “degree of orthotropy” of the material.

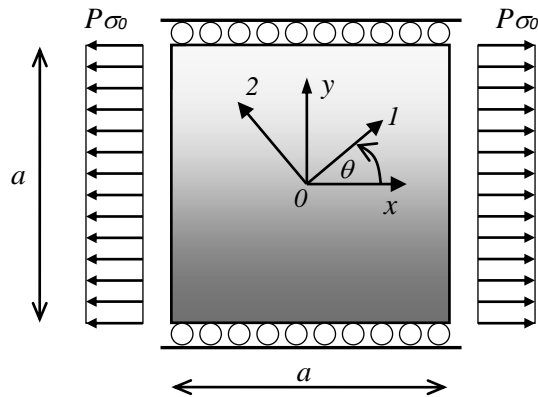


Fig. 7. Example #3: square plate, made of a tetratropic material, uniformly loaded along two opposite edges.

Looking at the mechanical model depicted in Fig. 7, the square plate of side a is uniformly loaded along two opposite edges in the x direction (at $x=\pm a/2$), while roller supports are applied along the other opposite edges in the y direction (at $y=\pm a/2$) so as to prevent transverse displacements of the plate. The load per unit length is specified as $P\sigma_0$, where σ_0 is a given reference stress value and P is a scalar load multiplier.

The plate is referred to a Cartesian co-ordinate system (x, y) while the principal directions of orthotropy are individuated by the Cartesian axes $(1, 2)$. The angle θ defines the counterclockwise angle between axis 1 and axis x along which the uniformly distributed load is applied (i.e. it indicates the fiber direction

of the laminate). As stated above, the material is tetratropic which implies that $X_c \equiv Y_c$ and $X_t \equiv Y_t$. According to the study carried out in [9], a parametric analysis has been performed in which the effect of the ratio between tensile and compressive strength as well as of the material degree of orthotropy is carefully investigated. The Tsai–Wu criterion, Eq. (12), is adopted but assuming the following expressions for the coefficients F_i and F_{ij} ($i, j = 1, 2, 6$):

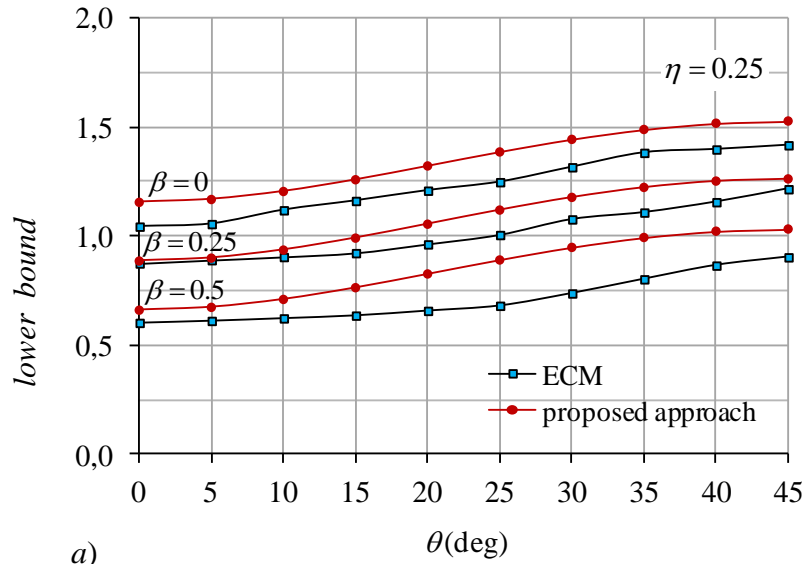
$$\begin{aligned} F_{11} = F_{22} &= \frac{1}{1-\beta^2} \frac{1}{\sigma_0^2}, & F_{66} &= 3\eta \frac{1}{1-\beta^2} \frac{1}{\sigma_0^2}, \\ F_{12} &= -\frac{1}{2(1-\beta^2)} \frac{1}{\sigma_0^2}, & F_1 = F_2 &= \frac{\beta}{1-\beta^2} \frac{1}{\sigma_0}, \end{aligned} \quad (19)$$

where β is the ratio between tensile and compressive material strength such that it represents the *degree of symmetry* of the material behavior ($\beta = 0$ corresponds to a symmetric behavior), whereas η defines the *degree of orthotropy* of the material (isotropy is recovered for $\eta = 1$). Note that only for $-1 < \beta < 1$ the yield surface (12) with coefficients given by (19) represents a convex domain. Note also that the value of σ_0 does not affect the solution since the coefficients reported in (19) are normalized by σ_0 .

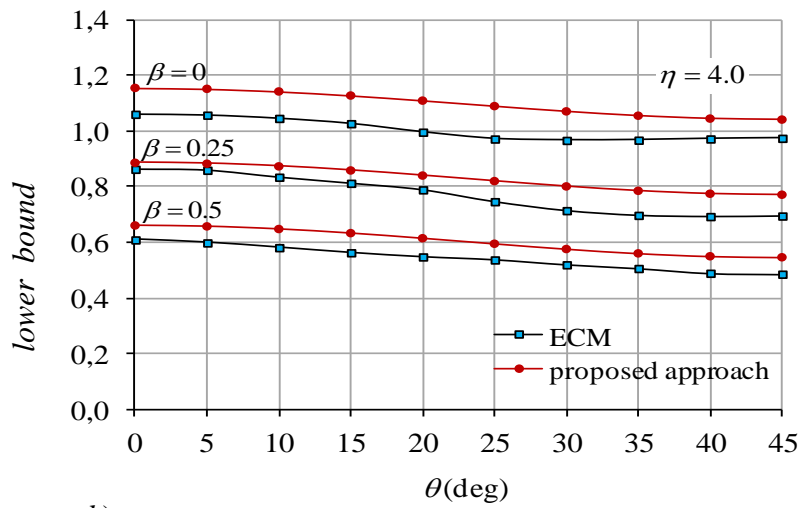
In order to check the reliability of the proposed limit analysis approach a comparative study has been performed with the results obtained by a different limit-analysis procedure, namely the Elastic Compensation Method. The ECM was originally conceived by Mackenzie and Boyle [31] for von Mises type materials, typically perfectly plastic steel materials, but its flexibility and

applicability have since been extensively demonstrated in literature for a much wider range of material laws (see e.g. [32], [33]). For completeness, only a few quite general concepts concerning this procedure are described hereafter. Basically, the ECM is an iterative procedure based on the static approach of limit analysis and therefore enables one to calculate a lower bound to the collapse load. The purpose of such numerical procedure is to build a statically and plastically admissible stress field for the structure, and this is achieved by performing a series of linear elastic FE-based analyses with adaptive elastic parameters that are iteratively adjusted. While performing the elastic analyses, highly loaded regions of the structure (defined by a certain number of FEs) are systematically weakened by reduction of the local modulus of elasticity in order to simulate a stress redistribution arising within the structure before attaining its limit-state threshold. To identify the critical FEs which are the ones where the elastic parameters are to be updated, the elastic stress value in each FE, say σ^e , is compared to the yield stress of the material, say σ^Y , only when $\sigma^e > \sigma^Y$ the reduction of the elastic moduli is put into effect. It appears clear that, even if based on the static approach of limit analysis, the ECM is to be considered rather different from the proposed limit analysis approach described in Section 2: the optimization problem, in fact, is not solved explicitly (i.e. in a strict mathematical way resorting to a mathematical programming algorithm), but using conventional FEM as the basis for an iterative procedure (the ECM belongs, in fact, to the so-called modulus

variation procedures similarly to the Linear Matching Method [14], [16], [18], [34]).



a)



b)

Fig. 8. Lower bound multipliers for the problem of Fig. 7: comparison between results obtained by the ECM and by the proposed approach for different θ , β and η values.

As far as this study is concerned, the problem sketched in Fig. 7 has been solved by an extension of the ECM to orthotropic composite laminates, the analytical details of which may be found in [25] and [15]. The Tsai–Wu failure criterion, Eq. (12), has been implemented as yield condition as explained in [15] and the FE elastic analyses, representing the iterations of the ECM, have been performed using the ADINA FE-code; a FORTRAN main program has been developed to drive the iterative procedure realizing the redistribution process throughout the laminate (in practice the updating of the elastic moduli to be used as input data in the FE-code at each new iteration).

Due to the symmetry of the problem only half of the plate has been studied in the FE-model, inserting the proper boundary conditions along the center line $x=0$. A FE-mesh consisting of 50 isoparametric 16 nodes quadrilateral elements has been considered with 16 Gauss points per element. The elastic moduli for the FE analyses are derived from the coefficients given in Eq.(19) and assumed as:

$$E_1 = \frac{1}{2F_{11}}, \quad E_2 = \frac{1}{2F_{22}}, \quad G_{12} = \frac{1}{2F_{66}}, \quad \nu_{12} = \frac{-F_{12}}{F_{22}} \quad (20)$$

In Fig. 8a, b the results given by the proposed static approach are compared with those obtained by the ECM. These two plots illustrate the lower bound multiplier, P_{LB} , versus the θ angle (i.e. for different fiber orientations with respect to the loading direction, see again Fig. 7) and for different β and η values; more specifically, three series of plots, $\beta=0, 0.25, 0.5$, are depicted in Fig. 8a, b for $\eta=0.25$ and $\eta=4.0$, respectively. If $\bar{\tau}$ is the maximum shear strength of the

laminate for the isotropic case, the latter two values of η , namely $\eta=0.25$ and $\eta=4.0$, corresponds to a maximum shear strength value equal to $2\bar{\tau}$ and $\bar{\tau}/2$, respectively. Moreover, since the material behavior in the two orthotropic directions is the same, only the interval $0^\circ \leq \theta \leq 45^\circ$ is studied; the maximum effect of anisotropy is obviously experienced for $\theta=45^\circ$. Overall, 60 different laminate cases have been analyzed in this comparative study.

By inspection of Fig. 8a, b it can be observed that the results obtained by the two different limit analysis approaches show a highly satisfactory correlation for all the examined laminate parameters. The collapse multiplier seems to depend linearly on β and the diagrams undergo a simple translation upon varying such β value. Relative differences of approximately 5-10% are noticed between the two approaches for all the considered cases, which is a really good result. It is worth noting that assuming a linear stress field within the proposed static approach—as the one expressed by Eq. (3)—produced the same collapse load multipliers as those obtained by assuming a constant stress field, which may be due to the simplicity of the studied loading condition or material properties.

As last numerical case analyzed, the mechanical model of example #4 is reported in Fig. 9. As can be seen, the same geometry as the previous example #3 has been considered, i.e. a square plate having side a (assumed equal to 10cm in this example) and unit thickness. In this example the plate is made, by hypothesis,

of a unidirectional orthotropic laminate with fibers directed along the x axis (i.e. $\theta=0^\circ$, $\underline{e}_1 \equiv \underline{e}_x$ and $\underline{e}_2 \equiv \underline{e}_y$).

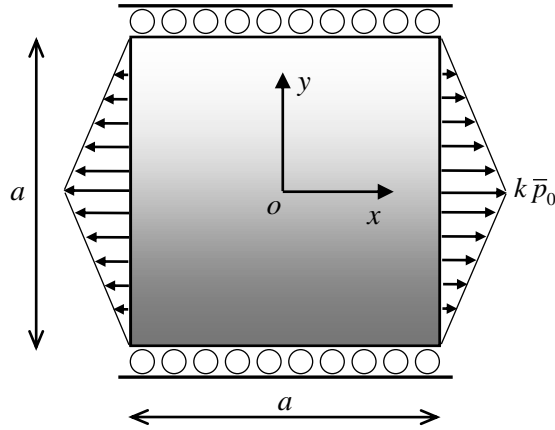


Fig. 9. Example #4: square plate, made of a unidirectional laminate with fibers parallel to x axis, subjected to a triangular tensile load distribution.

As a further difference compared to the previous example, the plate is loaded along two opposite edges in the x direction (at $x=\pm a/2$) by a triangular shaped distributed (not uniform) load, while the transverse displacements (along y) are prevented on the other edges (at $y=\pm a/2$) similarly to the previous example. The triangular load distribution is specified by its maximum value $k \bar{p}_0$ at $y=0$, where \bar{p}_0 is a given reference value (assumed equal to 20MN/cm) and k is a scalar load multiplier.

Two different composite materials have been considered, namely graphite/epoxy (T300/5208) and boron/epoxy (B(4)/5505). The material parameters of these two orthotropic laminates, in terms of strength values and elastic properties, are reported in Table 2.

Table 2. Example #4: mechanical parameters of the unidirectional orthotropic laminates of Fig. 9

T300/5208 graphite/epoxy laminate					
Elastic moduli (GPa) and Poisson ratio	E_1	E_2	G_{12}	ν_{12}	
	181	10.3	7.17	0.28	
Strength (MPa)	X_t	X_c	Y_t	Y_c	S
	1500	1500	40	246	68
B(4)/5505 boron/epoxy laminate					
Elastic moduli (GPa) and Poisson ratio	E_1	E_2	G_{12}	ν_{12}	
	221	20.7	5.79	0.23	
Strength (MPa)	X_t	X_c	Y_t	Y_c	S
	1260	2500	61	202	67

Also in this case the results obtained by the proposed static approach have been compared with those given by the ECM. With regard to the ECM, the same FE-mesh as example #3 has been adopted; nearly ten iterations (FE elastic analyses) were sufficient to obtain a convergent lower bound value. On the other hand, with regard to the proposed static approach the theoretical background given in Section 2 remains valid, but the stress field must be rectified in order to respect the loading conditions. Since the present test is uniaxial, the components of the stress field are:

- $\sigma_{xz}(\underline{X})$, $\sigma_{yz}(\underline{X})$ and $\sigma_{zz}(\underline{X})$ remain equal to zero due to the assumption of thin plate;

- $\sigma_{xx}(\underline{X})$ is taken a linear function of both x and y to satisfy the boundary conditions, $\sigma_{xx}\left(0, \frac{a}{2}\right) = \sigma_{xxa}$ and $\sigma_{xx}\left(\frac{a}{2}, \frac{a}{2}\right) = 0$, as given by Eq. (21).

$$\sigma_{xx}(\underline{X}) = \frac{\sigma_{xxa} - \sigma_{xx0}}{\frac{a}{2}} x - \frac{\sigma_{xxa}}{\frac{a}{2}} y + \sigma_{xx0}, \quad \forall \underline{X} \in \left[0, \frac{a}{2}\right] \times \left[0, \frac{a}{2}\right] \times \left[-\frac{h}{2}, \frac{h}{2}\right] \quad (21)$$

where σ_{xx0} and σ_{xxa} are the stress value in the center of the plate and at the edge $x=a/2$, respectively, and h is the plate thickness.

Table 3. Lower bound multipliers for the problem of Fig. 9: comparison between results obtained by the ECM and by the proposed approach for two orthotropic laminate types.

Laminate type	Lower bound multiplier	
	ECM	proposed approach
T300/5208 graphite/epoxy laminate	0.6962	0.6528
B(4)/5505 boron/epoxy laminate	0.9041	0.8410

The lower bound multipliers obtained by the two numerical procedures are reported in Table 3. Also for this example, a really good correlation is observed which demonstrates that the proposed approach is quite reliable in determining the collapse load multiplier; nevertheless, this example highlights that proper hypotheses on the mathematical expression of the stress field must be made, depending on the loading case studied, so as to allow a realistic description of the stress field inside the laminate. Such choice is, obviously, dictated by a plausible shape of the stress field and it should be reasonably made beforehand, which could appear a weakness point of the procedure. In spite of that, the examples run in this paper have shown that in many cases no significant difference is obtained by varying the stress field description; moreover, the simplicity of the optimization problem (18) to be solved renders the proposed static approach a

quite versatile and easy-to-handle numerical tool to face quite general biaxial loading cases as clearly confirmed by the accurate results obtained.

4. CONCLUSIONS

A limit analysis approach aimed to the prediction of a lower bound to the collapse load multiplier of composite laminates has been presented. The developed theory considers orthotropic composite laminates under axial and biaxial loading and plane stress conditions.

The key feature of this approach lies in the assumption of an appropriate, simple distribution of the stress field for each lamina inside the domain and, subsequently, in the solution of a nonlinear optimization problem driven by a standard optimization procedure. The choice of the approximate stress field described in this paper, which reduces the number of the optimization variables, together with the convexity of the failure criterion adopted at lamina level has the advantage of significantly reducing the computational effort related to the maximization problem. As a result, the proposed approach turns out to be very effective and computationally competitive if compared to other limit analysis numerical procedures. In this way the quoted approach appears simple to be utilized for practical applications.

The proposed approach has been validated, with reference to four examples, by comparing the predicted failure values in two cases with the ones (experimental) provided by a famous benchmark (WWFE) and for the other two

cases with those obtained by an alternative, well established, limit analysis procedure (ECM).

The obtained results witness how the proposed lower bound approach can be considered reliable at least for the examined cases. The encouraging results suggest to extend the application of the limit analysis procedure also to structural elements having more complex geometry and subjected to different load conditions.

REFERENCES

- [1] Jones RM. *Mechanics of Composite Materials*. 2nd ed. Philadelphia (PA, USA): Taylor & Francis Inc.; 1999.
- [2] Hinton MJ, Kaddour AS, Soden PD. A comparison of the predictive capabilities of current failure theories for composite laminates, judged against experimental evidence. *Composites Science and Technology* 2002; **62**: 1725-1797.
- [3] Icardi U, Locatto S, Longo A. Assessment of recent theories for predicting failure of composite laminates *Applied Mechanics Reviews ASME* 2007; **60** (2) : 76-86.
- [4] Soden P. Predicting the strength of composite laminates. *Reinforced Plastics* 2005; **49**(2), 42-48.
- [5] Xianfei Z, Yunwen F, Yuansheng F. Development research of failure theories for thick composite laminates, *Advanced Materials Research* 2012; **415-417**: 347-352.
- [6] Soden PD, Hinton MJ, Kaddour AS. Biaxial test results for strength and deformation of a range of E-glass and carbon fiber reinforced composite laminates: failure exercise benchmark data. *Composites Science and Technology* 2002; **62**:1489-1514.
- [7] Soden PD, Hinton MJ, Kaddour AS. Lamina properties and lay-up configurations and loading conditions of a range fiber reinforced composite laminates. *Composites Science and Technology* 1998; **58**(7):1011-1022.
- [8] Radenkovic D. Théorèmes limites pour un matériau de Coulomb à dilatation non standardisée. *CR Acad Sci Paris* 1961; **252**: 4103–4104.
- [9] Capsoni A, Corradi L, Vena P. Limit analysis of anisotropic structures based on the kinematic theorem. *International Journal of Plasticity* 2001; **17**:1531–1549.
- [10] Corradi L, Vena P. Limit analysis of orthotropic plates. *International Journal of Plasticity* 2003; **10**:1543–1566.
- [11] Francescato P, Pastor J. Lower and upper numerical bounds to the off-axis strength of unidirectional fiber-reinforced composite by limit analysis method. *Eur J Mech A: Solids* 1997; **16**: 213-234.

- [12] Limam O, Foret G, Ehrlacher A. Ultimate strength of free-edge composite laminates under tensile loading: a limit analysis approach. *Composites Part B* 2006; **37**: 286-291.
- [13] Limam O, Foret G, Zenzri H. Ultimate strength of pin-loaded composite laminates: a limit analysis approach. *Composite Structures* 2011; **93**:1217–24.
- [14] Chen HF, Ponter ARS. Shakedown and limit analyses for 3-D structures using the linear matching method. *Int J Press Vessels Piping* 2001 **78**(6):443–451.
- [15] Pisano AA, Fuschi P, De Domenico D. A layered limit analysis of pinned-joints composite laminates: Numerical versus experimental findings. *Composites Part B* 2012; **43**: 940-952.
- [16] Pisano AA, Fuschi P, De Domenico D. Failure modes prediction of multi-pin joints FRP laminates by limit analysis. *Composites Part B* 2013; **46**: 197-206.
- [17] Pisano AA, Fuschi P. Mechanically fastened joints in composite laminates: Evaluation of load bearing capacity. *Composites Part B* 2011; **42**: 949-961.
- [18] Pisano AA, Fuschi P. A numerical approach for limit analysis of orthotropic composite laminates. *International journal for numerical methods in engineering* 2007; **70**: 71-93.
- [19] Pisano AA, Fuschi P, De Domenico D. Peak load prediction of multi-pin joints FRP laminates by limit analysis. *Composite Structures* 2013; **96**: 763-772.
- [20] Bouabid A, Limam O. Etablissement d'une enveloppe bi-axiale à la rupture des composites stratifiés: Approche statique de type analyse limite. *Revue des composites et des matériaux avancés* 2011; **21**: 209-220.
- [21] Weichert D, Ponter ARS. *Limit states of materials and structures – Direct Methods*. Springer; 2009.
- [22] Spiliopoulos K, Weichert D. *Direct Methods for Limit States in Structures and Materials*. Dordrecht: Springer Science+Business Media B.V., 2013.
- [23] Fuschi P, Pisano AA, Weichert D. *Direct Methods for Limit and Shakedown Analysis of Structures Advanced Algorithms and Computational Material Modelling*. Springer Cham Heidelberg New York Dordrecht London © Springer International Publishing Switzerland DOI: 10.1007/978-3-319-12928-0, 2015.
- [24] Tsai SW, Wu EM. A general theory of strength for anisotropic materials. *Journal of Composite Materials* 1971; **5**:58–80.
- [25] Maple User Manual, version 12, 2010.
- [26] Soden PD, Kitching R, Tse PC. Experimental failure stresses for $\pm 55^\circ$ filament wound glass fiber reinforced plastic tubes under biaxial loads. *Composites* 1989; **20**: 125-135.
- [27] Soden PD, Kitching R, Tse PC, Tsavalas Y, Hinton MJ. Influence of winding angle on the strength and deformation of filament wound composite tubes subjected to uniaxial and biaxial loads. *Composites Science and Technology* 1993; **46**: 363-378.
- [28] Kaddour AS, Soden PD, Hinton MJ. Failure of $\pm 55^\circ$ filament wound composite tubes under biaxial compression. *J Compos Mater* 1998; **32**(18): 1618–45.
- [29] Hütter U, Schelling H, Krauss H. An experimental study to determine failure envelope of composite materials with tubular specimen under combined loads and comparison between several classical criteria. In: *Failure Modes Of Composite Materials With Organic Matrices And Other Consequences On Design*, NATO, AGRAD, Conf Proc No. 163, Munich, Germany, 13–19 October 1974.

- [30] Al-Khalil MFS, Soden PD, Kitching R, Hinton MJ. The effects of radial stresses on the strength of thin-walled filament wound GRP composite pressure cylinders. *Int J Mech Sci* 1996; **38**(1): 97-120.
- [31] Mackenzie D, Boyle JT. A method of estimating limit loads by iterative elastic analysis. Parts I, II, III. *International Journal of Pressure Vessels and Piping* 1993; **53**:77–142.
- [32] Pisano AA, Fuschi P, De Domenico D. Peak loads and failure modes of steel-reinforced concrete beams: Predictions by limit analysis. *Engineering Structures* 2013; **56**: 477-488.
- [33] De Domenico D, Pisano AA, Fuschi P. A FE-based limit analysis approach for concrete elements reinforced with FRP bars. *Composite Structures* 2014; **107**: 594-603.
- [34] Ponter ARS, Carter KF. Limit state solutions, based upon linear elastic solutions with spatially varying elastic modulus. *Computer Methods in Applied Mechanics and Engineering* 1997; **140**:237–258.